Dalton Transactions

ROYAL SOCIETY OF CHEMISTRY

PAPER

View Article Online
View Journal | View Issue

Cite this: *Dalton Trans.*, 2025, **54**, 13632

Synthesis and characterization of Sn(II) complexes supported by amino bis-phenoxide ligands

Aidan Ryan,[a] Hugo Delattre,[a] Gabriele Kociok-Köhn[b] and Andrew L. Johnson*[a]

Received 19th June 2025,
Accepted 5th August 2025

DOI: 10.1039/d5dt01442e

rsc.li/dalton

The coordination behavior of a series of [Sn(OR)$_2$] systems modified by substituted amine-bis(phenolate) ligands was investigated. The complexes were synthesised from the reaction of Sn[N(SiMe$_3$)$_2$]$_2$ and the appropriate pro-ligand: *N*,*N*-bis(3,5-dimethyl-2-hydroxybenzyl)ethylamine (**L^{1}H$_2$**), *N*′,*N*′-bis(2-hydroxy-3,5-dimethylbenzyl)-*N*,*N*-dimethylethylenediamine (**L^{2}H$_2$**), *N*,*N*′-bis(3,5-dimethyl-2-hydroxyphenylmethyl)-*N*,*N*′-dimethylethylenediamine (**L^{3}H$_2$**), 1,4-bis(2-hydroxy-3,5-dimethylbenzyl)-1,4-diazepane (**L^{4}H$_2$**), 2,2′,4,4′-tetramethyl-6,6′-piperazine-1,4-diylbis(methylene)-bisphenol (**L^{5}H$_2$**) and *N*′,*N*′,*N*″,*N*″-tetrakis(2-hydroxy-3,5-dimethylbenzyl)-1,2-ethanediamine, and the products were identified as follows: [{L^1}Sn]$_2$ (**1**), [{L^2}Sn] (**2**), [{L^3}Sn] (**3**), [{L^4}Sn], (**4**) and [{L^6}Sn$_2$]·(Py)$_2$ (**5**). Reaction of complex (**1**) with O$_2$ results in the formation of the Sn(IV) species [{L^1}$_2$Sn] (**6**), the molecular structure of which was also determined.

Introduction

Research into low-valent tin compounds has received significant attention since the isolation of the first persistent stannylene system of the type SnX$_2$ in 1973, *i.e.*, [Sn{CH(SiMe$_3$)$_2$}$_2$].[1] Since then, the chemistry of stannylenes has been investigated extensively with respect to their reactivity, molecular structures, bonding, coordination chemistry, and the possible applications of these heavy carbene analogues in catalysis and the construction of new functional materials.[2–7] More recently, molecular complexes of tin(II) have been investigated for their various applications in the activation of small molecules.[8–11]

Even though stannylenes, based on alkyl, aryl, and amide/phosphide, silyl and thiolate ligands have been isolated, tin(II) complexes based on aryloxide ligands are uncommon in contrast. Type **A** are aryloxides without additional intramolecular coordination Sn(OAr′)$_2$ (*e.g.*, Ar′ = 4-Me-C$_6$H$_4$, 2-^{i}Pr-C$_6$H$_4$, 2,6-^{i}Pr$_2$C$_6$H$_3$ 2,6-^{t}Bu$_2$C$_6$H$_3$, 2,6-^{t}Bu$_2$-4-Me-C$_6$H$_2$, 2,4,6-^{t}Bu$_3$C$_6$H$_2$, 2,6-Mes$_2$-C$_6$H$_3$),[12–16] stabilized by electronic (donation of a lone electron pair of oxygen) and steric (large aryl groups) effects (Fig. 1). While these species can range between monomeric, dimeric or oligomeric, this depends significantly on the steric influence of the aryloxide ligands; for example, while [Sn(OAr′)$_2$]$_x$ (Ar′ = 4-Me-C$_6$H$_4$; $x = \infty$ and 2-^{i}Pr-C$_6$H$_4$; $x = 4$) are oligomeric, sterically more encumbered systems, Sn(OAr′)$_2$ (Ar′ = 2-^{t}Bu-C$_6$H$_4$ or 2,6-Me$_2$-C$_6$H$_3$ and 2,6-^{i}Pr$_2$-C$_6$H$_3$)[16] complexes, are dimeric or monomeric (Ar′ = 2,6-^{t}Bu$_2$-4-Me-C$_6$H$_2$, 2,6-dipp-C$_6$H$_3$, OC$_6$H$_3$-^{t}Bu$_2$-2,6 or OC$_6$H$_2$-^{t}Bu-2,6-Me-4).[12–15] The second type (**B–M**) are complexes stabilized by the intramolecular interaction of a Sn atom by a Lewis basic group or lariat arm (Fig. 1). One of the possibilities for additional stabilization is achieved by the introduction of phenols containing donor groups, *e.g.*, amino-bisphenols (**B**) which have been isolated in the monomeric state due to the steric and electronic stabilization of the Sn(II) centre.[17–21] Other donor groups include

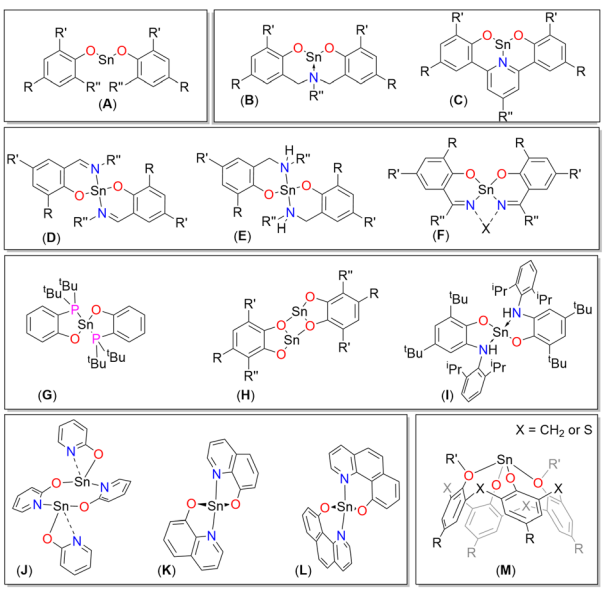

Fig. 1 Examples of tin(II) complexes bearing aryloxide ligands.

[a]*Department of Chemistry, University of Bath, Claverton Down, Bath. BA2 7AY, UK. E-mail: a.l.johnson@bath.ac.uk*
[b]*Materials and Chemical Characterisation Facility, University of Bath, Bath BA2 7AY, UK*

pyridyl groups (**C**),[22] imine groups (**D**),[23–25] amino groups (**E**),[26,27] and dianionic salen-and salen-like tetradentate chelator ligands (**F**) [salen = ethylene-*N*,*N*′- bis(salicylideneimine)] are also known.[28–31] Additionally, Sn(II) systems supported by ligands such as 2-phosphinophenolate (**G**),[32] catecholate (**H**),[33,34] aminophenolate(**I**), hydroxypyridine, benzoquinone and hydroxybenzo[*h*]quinoline derivatives (**J–L**)[35] as well as calix(4)arene derivatives (**M**) have also been reported.[36–39]

Obviously, the ligand structure is a significant factor not only in the stabilisation of the structure and the coordination number of the Sn atom but also affects its ability to participate in reactions. Here, we report the synthesis and structural characterisation of a family of amino-bisphenol-supported stannylene systems.

Results and discussion

Synthesis of pro-ligands

The amine-bis(phenol) ligands are versatile and important ligands that can be prepared relatively straightforwardly from common benchtop synthetic methods. The coordination chemistry of these ligands is eminently rich, and the compounds have been exploited in numerous applications in applied coordination chemistry including mimicking the activity of biological compounds, catalysis and molecular magnetism.[40] Substituents at the phenolate rings as well as the position and nature of the side-chain donor are easily tuneable features; the denticity and bulkiness of the amine-bis(phenol) ligand, as well as different electronic and steric properties, augment the coordination abilities of the ligands and affect the final coordination geometry (Scheme 1).

The pro-ligands $\mathbf{L^1H_2}$–$\mathbf{L^6H_4}$ involved in this investigation differ primarily in the nature of the phenol linker units, which have been selected on the basis of their ability to provide adaptable coordination environments for the Sn(II) centres, such that $\mathbf{L^1}$ and $\mathbf{L^6}$ provide an [O^N^O] coordination environment, and $\mathbf{L^2}$–$\mathbf{L^5}$ provides potential [O^N^O–N] and [O^N^N^O] coordination environments. In all cases, the phenolic pro-ligands $\mathbf{L^1H_2}$, $\mathbf{L^2H_2}$, $\mathbf{L^3H_4}$, $\mathbf{L^4H_2}$, $\mathbf{L^5H_2}$ and $\mathbf{L^6H_2}$ are readily prepared by modified Mannich reactions (Scheme 2) between 2,4-dimethylphenol formaldehyde and selected primary or secondary amines, according to literature procedures: $\mathbf{L^1H_2}$,[41] $\mathbf{L^2H_2}$,[42] $\mathbf{L^3H_2}$,[43] $\mathbf{L^4H_4}$,[44] $\mathbf{L^5H_2}$,[45] and $\mathbf{L^6H_2}$.[46]

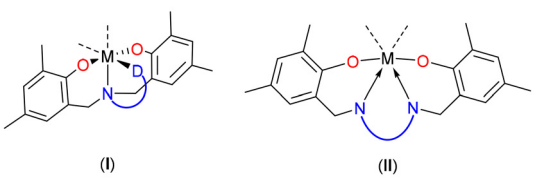

Scheme 1 Typical metal amine-bis(phenolate) coordination frameworks. (I) tri- or tetradentate amine bis(phenolate) system with a pendant arm (N–D) containing a lariat group (D); (II) Tetradentate amine bis(phenolate) system ligand with a diamino (N–N) bridge.

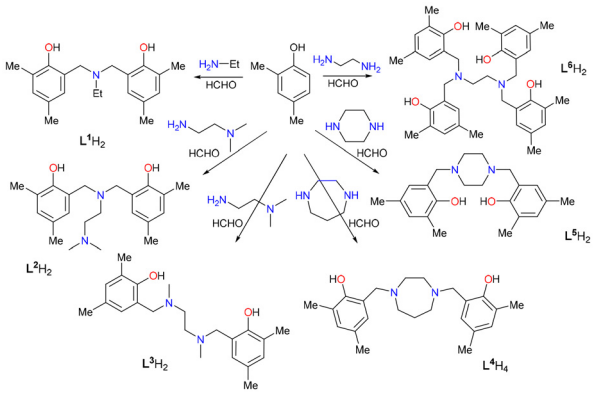

Scheme 2 Pre-ligands $\mathbf{L^1H_2}$–$\mathbf{L^5H_2}$ and $\mathbf{L^6H_4}$ used in this study.

The ligands were purified accordingly and characterised by comparison with literature data.

Synthesis of tin(II) complexes. In order to test the coordination behaviour, pro-ligands $\mathbf{L^1H_2}$, $\mathbf{L^2H_2}$, $\mathbf{L^3H_2}$, $\mathbf{L^4H_4}$ $\mathbf{L^5H_2}$ and $\mathbf{L^6H_2}$ were reacted with $[Sn\{N(SiMe_3)_2\}_2]$. The reaction of the pro-ligands $\mathbf{L^1H_2}$, $\mathbf{L^2H_2}$, $\mathbf{L^3H_2}$, and $\mathbf{L^4H_2}$ in a 1 : 1 ratio with $[Sn\{HMDS\}_2]$ in toluene resulted in an immediate colour change of the solutions from orange to pale yellow/colourless (Scheme 3).

Concentration *in vacuo* followed by hot filtration of the reaction mixture resulted in the formation of pale-yellow crystalline materials from the filtrate upon cooling to −15 °C. Complexes $[Sn\{\mathbf{L^1}\}]_2$ (**1**), $[Sn\{\mathbf{L^2}\}]$ (**2**), $[Sn\{\mathbf{L^3}\}]$ (**3**) and $[Sn\{\mathbf{L^4}\}]$ (**4**) were isolated by filtration and washed with cold hexane. Successive attempts to react the pro-ligand $\mathbf{H_2L^5}$ with one equivalent of $[Sn\{(HMDS)_2\}_2]$ in various solvents (toluene, diethyl ether, THF and

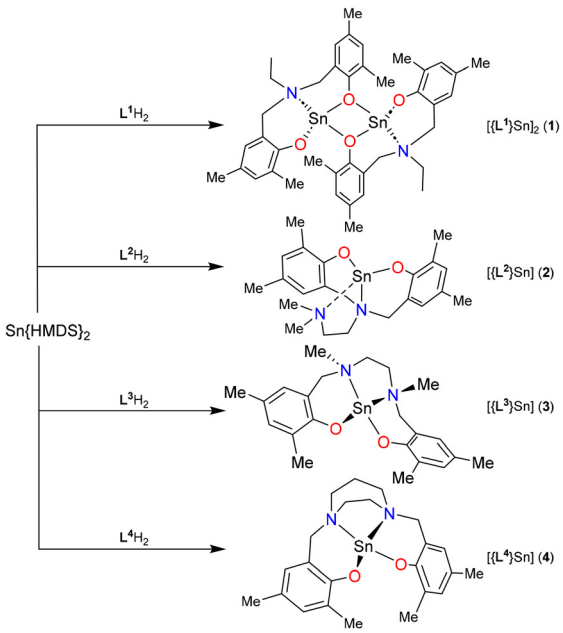

Scheme 3 Ligands and complexes prepared in this study.

pyridine) all resulted in the formation of intractable solids, immediately in the case of toluene and diethyl ether, and upon removal of the solvent in the case of THF and pyridine.

The reaction of the tetra-phenolic ligand $\mathbf{L^6H_4}$ with two equivalents of [Sn{HMDS}$_2$] resulted in a colour change and precipitation of an intractable colourless solid (Scheme 4). Attempts to dissolve the product in either THF or pyridine were unsuccessful. However, the reaction of two equivalents of [Sn{(HMDS)$_2$}$_2$] with $\mathbf{L^4H_4}$ in anhydrous pyridine resulted in the formation of a pale yellow solution. Removal of the pyridine solvent *in vacuo* followed by hot filtration from a toluene : THF mixture (5 : 1) resulted in the formation of pale yellow crystals of [Py$_2$·Sn$_2${$\mathbf{L^4}$}] (**5**) upon standing of the filtrate at 0 °C. Following recrystallisation, crystals of **1–4** were isolated cleanly in moderate to high yields (58–82%) and were characterised by solution state NMR (^{1}H, ^{13}C and ^{119}Sn) spectroscopy, single crystal X-ray diffraction and elemental analysis.

The ^{1}H and ^{13}C NMR spectra of complexes **1–4** were recorded in CD_2Cl_2 as an NMR solvent; both ^{1}H and ^{13}C NMR spectra of complexes **1–4** clearly show the absence of resonances associated with the {HMDS} ligands ($\sim\delta$ = 0.25 ppm) and are consistent with the formation of the homoleptic complexes. More informative are the ^{119}Sn NMR spectra for **1–4**, which show single resonances at δ = −431, −503, −454 and −475 ppm, respectively, indicating the isolation of a single reaction product with comparable Sn-coordination environments, as indicated by the ^{119}Sn chemical shifts. For complex **5**, NMR spectra were recorded in d$_5$-pyridine. Here the ^{1}H ^{13}C and ^{119}Sn NMR spectra again show the presence of a series of resonances associated with the tetra-phenolic ligand as indicated by the presence of resonances associated with two separate {^{t}Bu} groups, two triplet resonances associated with two separate phenolic {C–H} groups alongside two well-separated and defined 'AB' doublets for the {CH$_2$} protons and a single resonance at 3.50 ppm for the eight methyl hydrogen atoms of the {NCH$_2$CH$_2$N} group in an 18 : 18 : 2 : 2 : 2 ratio. This is consistent with molecular C_2-symmetry at the centre of the {NCH$_2$CH$_2$N} group. Additional resonances associated with coordinated pyridine are also observed in an approximate 5 : 1 ratio of pyridine to ligand. The ^{119}Sn NMR spectra showed a single resonance (in C_5D_5N) at δ = −532 ppm.

Molecular structures of complexes 1–4

Complexes **1–4** were characterized crystallographically and are shown in Fig. 2 (**1**) and Fig. 3 (**2–4**), respectively. Selected bond lengths and angles are given in Table 1. In the solid state, **1** crystallises in the triclinic space group $P\bar{1}$ with two independent dimer molecules in the asymmetric unit cell, as well as one molecule of toluene as a solvent of crystallisation. The ligand [**L1**] possesses three heteroatoms (2 oxygens and 1 nitrogen) and has been shown to be capable of binding to metals in either a terminal-[O^N^O] fashion[47] or as a bridging group in which the [O^N^O] ligand occupies both terminal and bridging positions.[48]

As can be seen from Fig. 2A the molecular structure of complex **1** (one of the two dimers in the unit cell is shown) is revealed to possess the latter of these structural motifs with oxygen atoms of a phenolate unit acting as a bridge between the two tin atoms, such that a *cis*-configured centrosymmetric dimeric structure with a central four-membered {Sn$_2$O$_2$} ring is formed *via* intermolecular O → Sn coordination of two stannabicyclodecane units, in a reminiscent of [Sn(OCH$_2$CH$_2$)$_2$NMe]$_2$

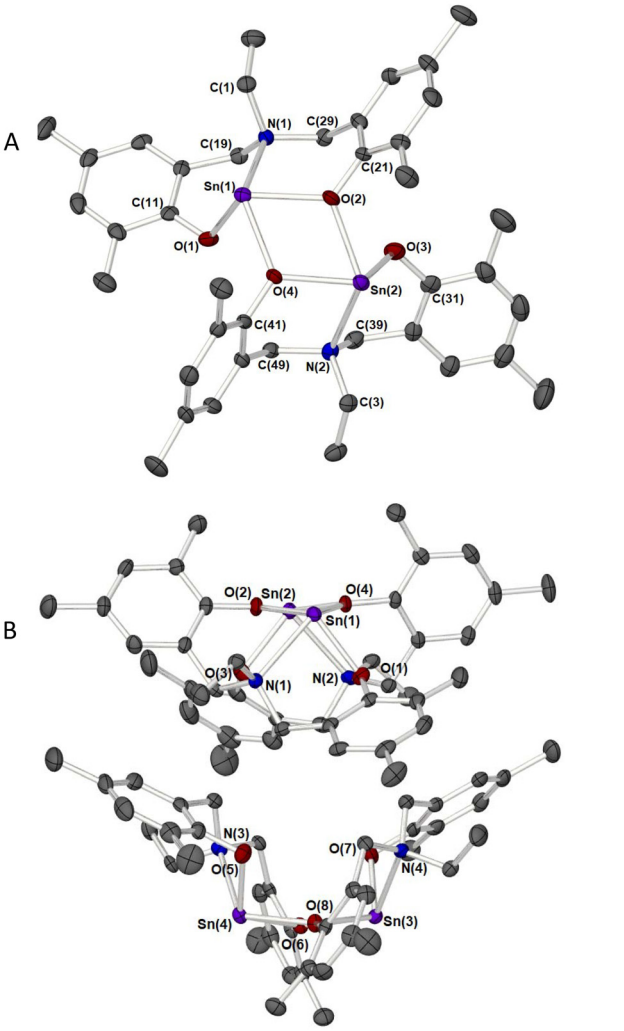

Fig. 2 (A) The molecular structures of one of the two dimer molecules in the unit cell of complex **1**, [{$\mathbf{L^1}$}Sn]$_2$. (B) Packing of the two molecular dimers in the unit cell. Thermal ellipsoids are shown at 50% probability. Hydrogen atoms are omitted for clarity.

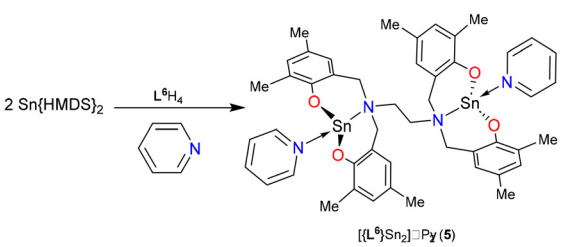

Scheme 4 Ligands and complexes prepared in this study.

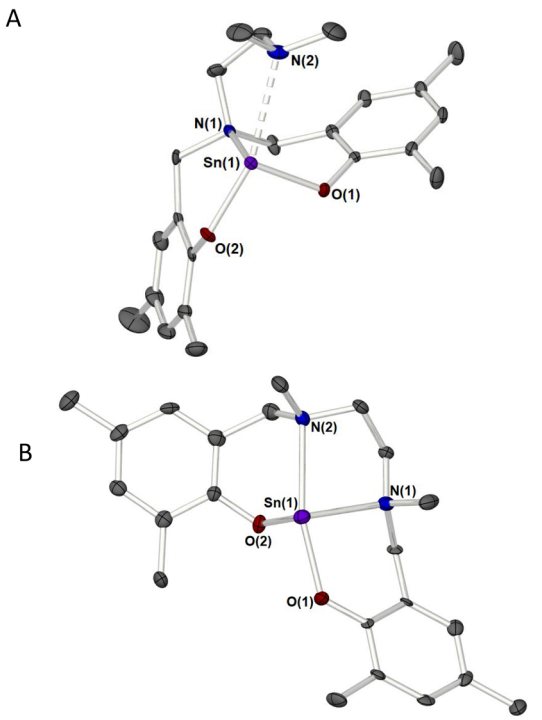

Fig. 3 The molecular structures of complexes **2**, [{L^2}Sn] (A), and **3**, [{L^3}Sn] (B), drawn with 50% probability ellipsoids. Hydrogen atoms are omitted for clarity.

and its derivatives,[49–51] to give 4-coordiante tin atoms with a *pseudo*-tetragonal pyramidal geometry. This is in contrast to the *ortho*-^{t}Bu derivative,[20] which is monomeric in the solid state, with a 3-coordinate Sn atom and subsequently shorter Sn–O and Sn ← N interactions.

At the core of the $\{Sn_2O_2\}$ ring, internal Sn–O interactions of 2.227(1) Å [Sn(1)–O(2)], 2.234(1) Å [Sn(1)–O(4)], 2.253(1) Å [Sn(2)–O(2)] and 2.200(1) Å [Sn(2)–O(4)] are augmented by terminal Sn–O interactions of 2.111(1) Å [Sn(1)–O(1)] and 2.098 (1) Å [Sn(2)–O(3)], as well as Sn → N interactions of 2.498(1) Å [Sn(1)–N(1)] and 2.522(1) Å [Sn(2)–N(2)], respectively, which complete the coordination of each Sn atom. As a result of the N → Sn coordination, the N(1) and N(2) atoms become chiral with (*R*) configurations.

Fig. 2B shows the relative arrangement of the two independent dimer molecules in the unit cell, down the approximate *c*-axis. Analysis of intermolecular contacts would suggest that the arrangement of the two dimer molecules is a result of packing effects.

In contrast to complex **1**, complexes **2–4** are all unimolecular and crystallise in the space groups $P2_1/n$ (**2**), *Pbca* (**3**) and $P2_1/c$ (**4**) respectively.

Single crystals of the stannylenes **2** and **3** suitable for X-ray diffraction analysis (Fig. 3) were grown from concentrated toluene solutions.

Ligands [L^2] and [L^3] possess four heteroatoms (2 oxygens and 2 nitrogens) with similar ligands having been shown to

Table 1 Single crystal X-ray diffraction experimental details for complexes **1–5**

Compound	**1**	**2**	**3**	**4**	**5**	**6**
Chemical formula	$C_{87}H_{108}N_4O_8Sn_4$	$C_{22}H_{30}N_2O_2Sn$	$C_{22}H_{30}N_2O_2Sn$	$C_{51}H_{65}N_5O_4Sn_2$	$C_{63}H_{69}N_7O_4Sn_2$	$C_{54}H_{66}N_2O_4Sn$
Formula Mass	1812.53	473.17	473.17	1049.46	1225.63	925.77
Crystal system	Triclinic	Monoclinic	Orthorhombic	Monoclinic	Monoclinic	Monoclinic
Space group	*P*	*P*21/*n*	*Pbca*	*P*21/*c*	*P*21/*n*	*P*21/*c*
a/Å	14.5961(4)	11.25310(10)	7.83230(10)	24.51991(12)	12.16953(8)	15.4186(2)
b/Å	14.6600(5)	14.09620(10)	15.26360(10)	12.63699(7)	21.43889(15)	21.9250(2)
c/Å	20.1553(5)	14.02500(10)	35.1984(3)	15.47487(9)	21.98942(15)	14.6746(2)
α/°	72.735(2)	90	90	90	90	90
β/°	83.418(2)	106.1290(10)	90	95.1081(5)	91.0062(6)	110.0141(15)
γ/°	88.995(2)	90	90	90	90	90
Unit cell volume/Å^3	4090.7(2)	2137.16(3)	4207.94(7)	4775.97(5)	5736.18(7)	4661.20(11)
Z (formula units per unit cell)	2	4	8	4	4	4
Crystal Size	0.32 × 0.21 × 0.15	0.34 × 0.23 × 0.18	0.23 × 0.13 × 0.02	0.46 × 0.09 × 0.05	0.76 × 0.07 × 0.06	0.62 × 0.47 × 0.28
Temperature/K	150(2)	150(2)	150(2)	150(2)	150(2)	150(2)
Space group	*P*	*P*21/*n*	*Pbca*	*P*21/*c*	*P*21/*n*	*P*21/*c*
Radiation type	Mo Kα	Cu Kα	Cu Kα	Cu Kα	Cu Kα	Cu Kα
Absorption coefficient, *μ*/mm^{-1}	1.264	9.649	9.801	8.703	7.345	4.725
No. of reflections measured	37 894	18 791	61 969	101 818	46 157	32 217
No. of independent reflections	18 348	4256	4207	9571	11 393	8988
R_{int}	0.0323	0.0295	0.0796	0.0452	0.0338	0.0379
Final R_1 values ($I > 2\sigma(I)$)	0.0368	0.0332	0.0843	0.0248	0.0225	0.0342
Final w$R(F^2)$ values ($I > 2\sigma(I)$)	0.0683	0.0897	0.1973	0.0647	0.0556	0.0944
Final R_1 values (all data)	0.0535	0.0335	0.0848	0.0255	0.0241	0.0353
Final w$R(F^2)$ values (all data)	0.0755	0.0900	0.1974	0.0653	0.0566	0.0955
Goodness of fit on F^2	1.026	1.078	1.268	1.055	1.027	1.070
CCDC number	2465593	2465589	2465592	2465594	2465591	2465590

support the formation of unimolecular complexes through binding to metals in a tetradentate terminal-$[O^{\cap}N^{\cap}O\text{–}N]^{2-}$ fashion,[52,53] as well as a bridging group in which the $[O^{\cap}N^{\cap}O\text{–}N]^{2-}$ ligand spans terminal and bridging positions through phenolate oxygen atoms.[42,54,55]

The central tin atom in **2** possesses a [3 + 1] coordination mode due to the formation of two transannular Sn ← N interactions (Fig. 3A): a strong bond with the bridgehead-amine N atom [Sn(1)–N(1) = 2.364(2) Å] and a weaker interaction with the N atom of the {NMe_2} lariat arm [Sn(1)–N(1) = 2.773(2) Å]. Similarly, the distances between the Sn(II) atom and the oxygen atoms are notably different; the Sn–O bonds are asymmetric, with short and long bonds [Sn(1)–O(1) = 2.069(3) Å, Sn(1)–O(2) = 2.103(3) Å]. As a result, the coordination environment of the Sn atom in **2** is best described as a 4-coordinate distorted pseudo-trigonal bipyramid [τ_{Sn} = 1.14: O(2)–Sn(1)–N(2) = 153.60(8)°, O(1)–Sn(1)–N(1) 84.98(8)°][56] with O(2) and N(2) occupying axial positions, and O(1) and N(1) the equatorial positions. A direct interpretation of the geometry about the tin atom would suggest that the tin center possesses a stereoactive lone pair of electrons. However, inspection of the bond angles about the Sn centre [O(1)–Sn(1)–O(2) = 92.84(8)°; O(2)–Sn(1)–N(1) = 85.07(7)°; N(1)–Sn(1)–N(2) = 70.307(7)°; O(1)–Sn(1)–N(1) = 92.84(8)°; O(1)–Sn(1)–N(2) = 94.29(7)°] would suggest a lack of hybridisation, *i.e.*, a 5s lone pair of electrons.

A very similar structural geometry is observed for the stannylene **3** (Fig. 3B) grown from *i.e.* a 4-coordinate distorted pseudo-trigonal bipyramid geometry about the Sn centre [τ_{Sn} = 0.94: O(1)–Sn(1)–N(2) = 149.8(3)°, O(2)–Sn(1)–N(2) = 93.7(3)°], with asymmetric Sn–O bonds [Sn(1)–O(1) = 2.069(3) Å, Sn(1)–O(2) = 2.103(3) Å] and Sn ← N interactions [Sn(1)–N(1) = 2.387(9) Å, Sn(1)–N(2) = 2.599(8) Å]. Similarly, angles at the Sn centre in **3** do not suggest hybridization at the metal centre [O(1)–Sn(1)–O(1) = 85.8(3)°; O(1)–Sn(1)N(1) = 92.84(8)°; O(2)–Sn(1)–O(2) = 85.07(7)°; N(1)–Sn(1)–N(2) = 73.1(3)°]. Both **2** and **3** have structural similarities to the bis(phenoxy)-amine tin(II) complexes reported by Zaitsev *et al.*[19] and Praban *et al.*[21]

As part of this study, the molecular structure of the {^{t}Bu} analogue of **3** was also isolated and collected. The molecular structure and full characterisation data are included in the SI.

Similarly, [L^4] acts as an $[O^{\cap}N^{\cap}N^{\cap}O]^{2-}$ coordinating ligand and has been shown to support the formation of unimolecular complexes.[45,57] In the case of complex **4**, the compound crystallises with two independent molecules in the monoclinic unit cell, one of which is shown in Fig. 4. As no substantial differences in bond lengths and angles are found between the two crystallographically non-equivalent molecules, only one ORTEP diagram for the structure of compound **4** is displayed in Fig. 4.

While the Sn–O bonds [Sn(1)–O(1) = 2.065(3) Å; Sn(1)–O(2) = 2.095(3) Å; Sn(2)–O(3) = 2.062(2) Å; Sn(2)–O(4) = 2.086(2) Å] and Sn ← N interactions [Sn(1)–N(2) = 2.402(2) Å; Sn(1)–N(1) = 2.478(2) Å; Sn(2)–N(4) = 2.405(3) Å; Sn(2)–N(3) = 2.523(3) Å] are comparable to those found in complexes **1–3**, there is an obvious reduction in the asymmetry of the bond lengths. This is concomitant with a change in the geometry of the stannylene: from a distinctly distorted pseudo-trigonal bipyramidal geometry in **2–3**, to a geometry between trigonal bipyramidal and square-based pyramidal in **4** [τ_{Sn} = 0.72/0.64: O(1)–Sn(1)–N(2) = 140.85(5)°, O(2)–Sn(1)–N(1) = 97.70(6)°, O(4)–Sn(2)–N(3) = 139.14(6)°, O(3)–Sn(2)–N(4) = 101.11(6)°], presumably a result of restricted flexibility in the homopiperazine backbone. The remaining angles in **4** show a greater deviation away from 90° (more acute) compared to comparable angles in **2** and **3** [O(1)–Sn(1)–O(2) = 85.74(6), O(2)–Sn(1)–N(2) = 82.45(5), O(1)–Sn(1)–N(1) = 77.71(5), N(2)–Sn(1)–N(1) = 65.28(5), O(3)–Sn(2)–O(4) = 84.62(6), O(3)–Sn(2)–N(4) = 101.11(6), O(4)–Sn(2)–N(4) = 83.75(6), N(4)–Sn(2)–N(3) = 64.68(6)].

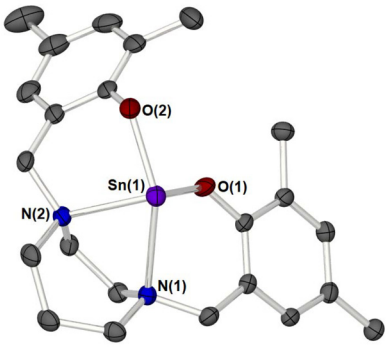

Fig. 4 The molecular structure of one of the two complexes in the unit cell of complex **4**, [{L^4}Sn], (50% probability ellipsoids). Hydrogen atoms and solvent of crystallisation (pyridine) are omitted for clarity.

In contrast to ligands **[L^1]–[L^5]**, ligand [L^6] possesses six heteroatoms (4-oxygens and 2-nitrogens) and has been shown to be capable of binding to metals in various modes dependent upon the degree of de/protonation in the ligand and the coordination demands of the metal.[18] Single crystal X-ray diffraction studies revealed that the product **5** comprises two independent halves of the tetraphenolate ligand coordinated to two Sn(II) in a tridentate $[O^{\cap}N^{\cap}O]^{2-}$ fashion, wherein the "N$(CH_2)_2$N" moiety also acts as a bridge to connect each Sn metal center. No substantial differences in bond lengths and angles are found between the two crystallographically non-equivalent half-molecules, as such only one ORTEP diagram for the structure of compound **5** is displayed in Fig. 5. Each Sn(II) is additionally coordinated by a pyridine molecule rendering each Sn(II) centre 4 coordinate, with distorted pseudo-trigonal bipyramidal geometries about the Sn centre [τ_{Sn} = 0.86: N(1)–Sn(1)–N(3) = 150.55(5)°, O(1)–Sn(1)–O(2) = 99.15(5)°], [N(2)–Sn(2)–N(4) = 147.67(5)°, O(5)–Sn(2)–O(6) = 100.99(5)°], with Sn–O bonds [Sn(1)–O(1) = 2.076(2) Å, Sn(1)–O(2) = 2.057(3) Å, Sn(2)–O(5) = 2.078(2) Å, Sn(2)–O(6) = 2.047(3) Å,] and Sn ← N interactions [Sn(1)–N(1) = 2.551(3) Å, Sn(2)–N(2) = 2.528(3) Å] which are similar to those found in **1–4**, with Sn ← pyridine interactions [Sn(1)–N(3) = 2.434(2) Å; Sn(2)–N(4) = 2.471(3) Å] which are comparable to those found in similar Sn(II) systems.[18] Again, angles about the Sn centres in **5** do not suggest hybridization at the metal centre [O(1)–Sn(1)–N(1) = 81.23(5)°; O(1)–Sn(1)–N(3) = 80.97(5)°; O(2)–Sn(1)–N(1) = 81.23(5)°; O(2)–Sn(1)–

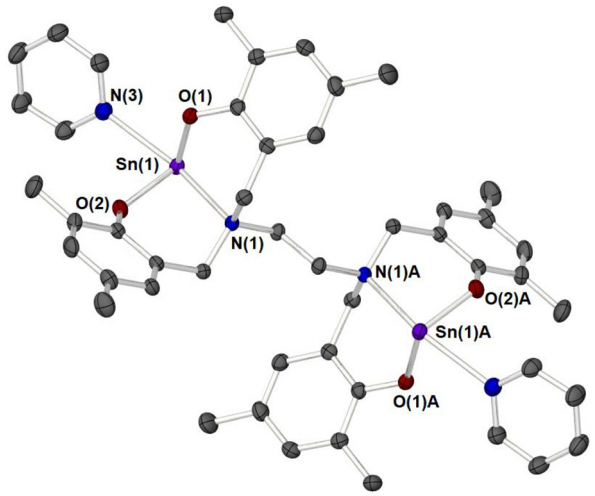

Fig. 5 Thermal displacement ellipsoid drawing (50% probability) showing one of the two [{L^6}Sn_2]·Py_2 half-molecules in the unit cell of **5**. Symmetry-generated atoms (A) generated by the symmetry operation (1 − *X*, 1 − *Y*, 1 − *Z*). All hydrogen atoms and solvent of crystallisation (pyridine) are omitted for clarity.

N(3) = 78.79(5)°; O(5)–Sn(2)–N(2) = 81.32(5)°; O(5)–Sn(1)–N(4) = 78.55(5)°; O(6)–Sn(1)–N(2) = 81.48(5)°; O(6)–Sn(1)–N(4) = 77.89 (5)°]. Three additional pyridine solvent molecules were also located in the unit-cell lattice.

Reactivity

To gain insight into the reactivity of these complexes, a simple redox reaction was attempted. Oxygen gas was bubbled through a toluene solution of complex **1** (Scheme 5). Addition of oxygen gas to the pale-yellow solution resulted in darkening of the solution and precipitation of an insoluble white solid. The solution was filtered, and the filtrate was evaporated to dryness. Recrystallisation from hot toluene yielded crystals of **6**, which were isolated cleanly in moderate to high yields (44% based on Sn) and were characterised by solution-state NMR (^{1}H, ^{13}C and ^{119}Sn) spectroscopy, single crystal X-ray diffraction and elemental analysis. The ^{1}H and ^{13}C NMR spectra of **6** (CD_2Cl_2 was used because of solubility issues) reveal a single set of resonances consistent with molecular C_1-symmetry, which are shifted with respect to those of complex **1**, indicating asymmetry of the ligand. The ^{119}Sn NMR spectra similarly showed a shift to δ = −670 ppm (*cf.* −431 ppm for **1**). We believe that the changes in the NMR spectra are indicative of a change in the oxidation state of the Sn centre from Sn(II) to Sn (IV). Single crystal X-ray diffraction studies reveal that the crystals, isolated from the reaction mixture, are the octahedral tin (IV) complex *trans*/*mer*-[{L^1}$_2$Sn], **6**. This is presumably the result of oxidation of **1** to form a putative "[{L^1}Sn═O]" species, which then undergoes ligand exchange to form **6** with expulsion of SnO_2, as a white solid (Scheme 5).

The molecular structure of **6** is shown in Fig. 6 and clearly shows that the overall geometry around the Sn(IV) atom is best described as a distorted meridional octahedron with the nitrogen atoms N(1) and N(2) of the amine bis(phenolate)-ligand {L^1} positioned *trans* to each other. The doubly deprotonated

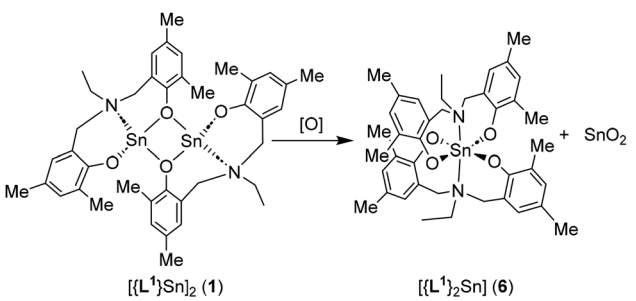

Scheme 5 Oxidative conversion of **1** into **6**.

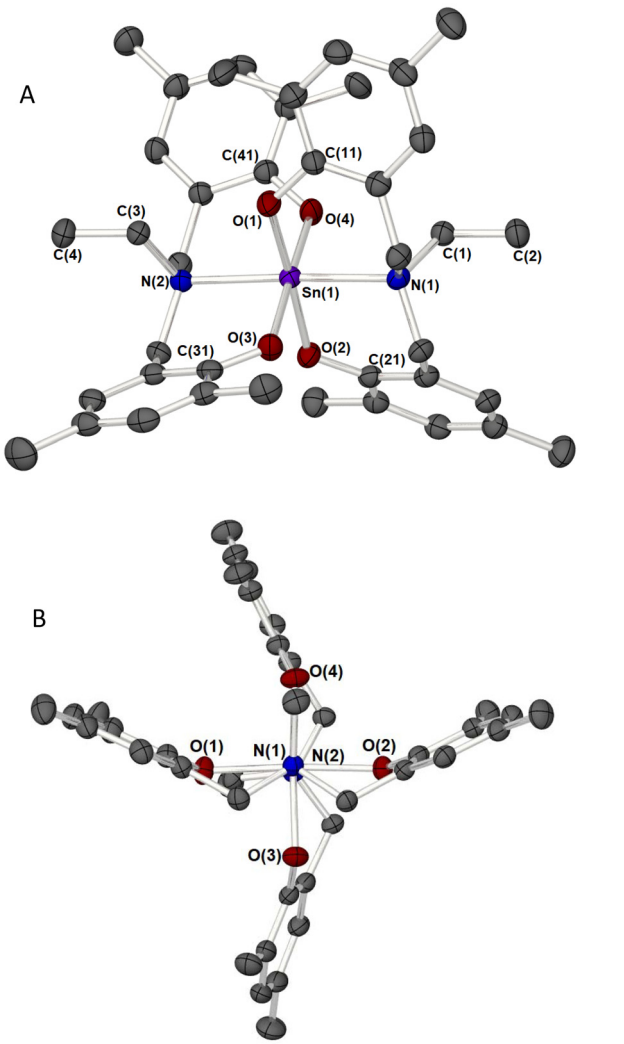

Fig. 6 (A) Thermal displacement ellipsoid drawing (50% probability) showing [{L^1}$_2$Sn] in the unit cell of **6**. (B) View of the molecule down the N(1)–Sn(1)–N(2) axis showing the relative orientation of the two tridentate amino-bis(phenolate) ligands, which coordinate to Sn(IV) in a meridional fashion. All hydrogen atoms and solvent of crystallisation (toluene) are omitted for clarity.

ligand, $[O^{\cap}N^{\cap}O]^{2-}$, is bound in a meridional fashion, with the facial mode being sterically unavailable. The distortion from an octahedral geometry is small in the $[ONO]^{2-}$ ligand: N(1)–Sn(1)–O(1) = 90.51(7), N(1)–Sn(1)–O(2) = 90.30(7)°, N(2)–Sn(1)–O(3) = 89.21(6)°, and N(2)–Sn(1)–O(4) = 90.79(6)°. The O(1)–Sn(1)–O(2) and O(3)–Sn(1)–O(4) angles are 176.49(7)° and 177.04(7)°, respectively, while the corresponding N(1)–Sn(1)–N(2) angle at 177.53(6)° deviates from linearity. The planarity of the $\{SnO_4\}$ fragment is exceedingly good; the maximum deviation from the mean plane is 0.008 Å. The average Sn–O and Sn–N distances of 2.021(3) and 2.238(3) Å fall in the range reported for the structurally characterized mononuclear Sn(IV) complexes.[58–60]

Similar structural systems have also been reported for homo- and heteroleptic $[O^{\cap}N^{\cap}O]$ complexes of titanium,[47,61,62] zirconium and hafnium.[63] Jones and co-workers also reported independently a series of structurally characterized homoleptic group 4 complexes of sterically less demanding $[O^{\cap}N^{\cap}O]$ ligands.[64]

The reactivity of complexes **2** and **3** toward molecular oxygen was also investigated during our study. In the case of complex **2**, reaction with O_2 in toluene resulted in the formation of a clear solution from which crystals of the proligand $\mathbf{L^2H_2}$ were isolated. However, this may have been the result of accidental exposure to moisture during prolonged standing. As such, the precise nature of the reaction, if any, is not clear; what is clear is that the ^{119}Sn NNR spectra of the as-reacted reaction mixture revealed the absence of Sn species in solution.

In the case of complex **3**, the attempted reaction with molecular O_2 in a toluene solution resulted in a slight clouding of the solution. Nonetheless, extraction and filtration, followed by recrystallisation, yielded crystals of **3**, indicating a lack of reactivity.

Experimental

Complexes **1–6** were synthesised under air- and moisture-sensitive conditions. All manipulations were carried out under an atmosphere of nitrogen or argon using standard Schlenk-line or glovebox techniques. Solvents were dried according to standard methods and collected by distillation. $[Sn(HMDS)_2]$ was produced according to a literature procedure.[65] The proligands $\mathbf{L^1}$–$\mathbf{L^5H_2}$ and $\mathbf{L^6H_4}$ were produced according to literature procedures.[41–46]

Synthesis of $[Sn\{L^1\}]_2$ (1). A toluene solution (5 ml) of $\mathbf{H_2L^1}$ (0.94 g, 3 mmol) was added to $Sn(HMDS)_2$ (1.318 g, 3 mmol) in toluene (5 ml), at 0 °C. The reaction mixture was left stirring for one hour, and the colour changed from orange to pale yellow. The solution was filtered to remove impurities. The filtrate was concentrated *in vacuo*, and the product was recrystallised from toluene. Yield = 0.95 g, 74%. ^{1}H NMR (400 MHz, CD_2Cl_2, 25 °C); δ_{ppm} 1.38 (t, $^3J_{HH}$ = 7.27 Hz, 6H, NCH_2Me), 2.18 (s, 12H, ArMe), 2.19 (s, 12H, ArMe), 2.97 (quartet, $^3J_{HH}$ = 7.27 Hz, 4H, NCH_2Me), 3.61 (s, 4H, $ArCH_2N$), 6.64 (d, $^4J_{HH}$ = 1.62 Hz, 4H, ArH), 6.93 (d, $^4J_{HH}$ = 1.62 Hz, 4H, ArH); $^{13}C\{^1H\}$ NMR (100 MHz); δ_{ppm} 9.8 (NCH_2Me), 17.0 (Ar–Me), 20.5 (Ar–Me), 50.8 (NCH_2Me), 55.0 (Ar–CH_2N), 122.7 (Ar–C), 127.2 (ArC), 129.2 (Ar–CH), 129.4 (Ar–CH), 132.5 (ArC), 155.6 (Ar–CO); ^{119}Sn NMR (186 MHz); δ_{ppm} −431; elemental analysis for $C_{40}H_{50}N_2O_4Sn_2$: calc. C, 55.85; H, 5.86; N, 3.26; Found C, 55.82; H, 5.88; N, 3.22.

Synthesis of $[Sn\{L^2\}]$ (2). A toluene solution (5 ml) of $\mathbf{H_2L^2}$ (0.36 g, 1 mmol) was added to $Sn(HMDS)_2$ (0.44 g, 1 mmol) in toluene (5 ml), at room temperature. The reaction mixture was left stirring for one hour, and the colour changed from orange to pale yellow. The solution was filtered to remove impurities. The filtrate was concentrated *in vacuo*, and the product was recrystallised from toluene (1 ml). Yield = 0.31 g, 66%. ^{1}H NMR (500 MHz, CD_2Cl_2, 298 K) δ_H: 1.90 (s, 6H, $N(CH_3)_2$), 2.14 (s, 6H, Ar–CH_3), 2.16 (s, 6H, Ar–CH_3), 2.46 (m, 2H, $NCH_2CH_2N(CH_3)_2$), 2.95 (m, 2H, $NCH_2CH_2N(CH_3)_2$), 3.64 (s, 4H, $ArCH_2N$), 6.57 (s, 2H, Ar–H), 6.88 (s, 2H, Ar–H); $^{13}C\{^1H\}$ NMR (125 MHz, CD_2Cl_2, 298 K) δ_C: 16.9 (Ar–CH_3), 20.5 (Ar–CH_3), 44.1 ($N(CH_3)_2$), 55.1 ($NCH_2CH_2N(CH_3)_2$), 57.6 ($NCH_2CH_2N(CH_3)_2$), 59.4 (Ar–CH_2N), 122.6 (Ar–C), 125.6 (Ar–C), 128.5 (Ar–C), 128.9 (Ar–CH), 132.1 (ArCH), 157.2 (Ar–CO) $^{119}Sn\{^1H\}$ NMR (186 MHz, CD_2Cl_2, 298 K) δ_{Sn}: −503; ^{119}Sn NMR (186, C_6D_6, MHz); δ_{ppm} −495; elemental analysis for $C_{22}H_{30}N_2O_2Sn{\cdot}C_6H_8$: calc. C, 60.78; H, 6.92; N, 5.06; Found C, 60.05; H, 5.95; N, 5.03.

Synthesis of $[Sn\{L^3\}]$ (3). A toluene solution (5 ml) of $\mathbf{H_2L^3}$ (0.36 g, 1 mmol) was added to $Sn(HMDS)_2$ (0.44 g, 1 mmol) in toluene (5 ml) at room temperature. The reaction mixture was left stirring for one hour, and the colour changed from orange to pale yellow. The solution was filtered to remove impurities. The filtrate was concentrated *in vacuo*, and the product was recrystallised from fresh toluene (5 mL) and THF (1 mL) at −25 °C. Yield = 0.19 g, 40%. ^{1}H NMR (500 MHz, CD_2Cl_2, 298 K) δ_H: 2.17 (s, 6H, NCH_3), 2.21 (s, 6H, $ArCH_3$), 2.25 (s, 6H, Ar–CH_3), 2.72 (q, J = 6.4 Hz, 2H, NCH_2CH_2N), 3.00–3.09 (m, 4H, $ArCH_2N$ and NCH_2CH_2N), 4.16 (s, 1H, Ar–CH_2N), 4.19 (s, 1H, Ar–CH_2N), 6.66 (s, 2H, Ar–H), 6.95 (s, 2H, Ar–H); $^{13}C\{^1H\}$ NMR (125 MHz, CD_2Cl_2, 298 K) δ_C: 17.1 (Ar–CH_3), 20.5 (Ar–CH_3), 42.0 (NCH_3), 55.8 (NCH_2CH_2N), 60.2 (Ar–CH_2N), 123.5 (Ar–C), 125.5(Ar–C), 128.8 (Ar–H), 129.3 (Ar–C), 131.7 (Ar–CH), 157.4 (Ar–CO); $^{119}Sn\{^1H\}$ NMR (186 MHz, CD_2Cl_2, 298 K) δ_{Sn}: −454; elemental analysis for $C_{22}H_{30}N_2O_2Sn$: calc. C, 55.84; H, 6.39; N, 5.92; Found C, 55.86; H, 6.23; N, 5.67.

Synthesis of $[Sn\{L^4\}]$ (4). $\mathbf{H_2L^4}$ (0.37 g, 1 mmol) in toluene (5 ml) was added to $Sn(HMDS)_2$ (0.44 g, 1 mmol) in toluene at 0 °C. The reaction mixture was left stirring for one hour, initially turning colourless, and later turning pale yellow. The solvent was removed *in vacuo* and replaced with fresh toluene (5 ml). The reaction mixture was then filtered hot (110 °C) through Celite to remove impurities. The reaction was concentrated *in vacuo*, and the product was recrystallised at −25 °C. Yield = 0.28 g, 58%. ^{1}H NMR (500 MHz, CD_2Cl_2, 298 K) δ_H: 2.10 (s, 6H, $ArCH_3$), 2.14 (s, 6H, $ArCH_3$), 2.20–2.35 (m, 2H, $NCH_2CH_2CH_2N$), 2.40–2.47 (m, 2H, NCH_2CH_2N), 2.55–2.62 (m, 2H, $NCH_2CH_2CH_2N$), 3.04 (s, 1H, Ar–CH_2N), 3.06 (s, 1H, Ar–CH_2N), 3.07–3.11 (m, 2H, NCH_2CH_2N), 3.27–3.36 (m, 2H, $NCH_2CH_2CH_2N$), 4.12 (s, 1H, $ArCH_2N$), 4.14 (s, 1H, $ArCH_2N$),

6.51 (s, 2H, Ar–H), 6.84 (s, 2H, Ar–H); $^{13}C\{^1H\}$ NMR (125 MHz, CD_2Cl_2, 298 K) δ_C: 17.3 (Ar–CH_3), 20.4 ($ArCH_3$), 24.4 ($NCH_2CH_2CH_2N$), 46.8 (NCH_2CH_2N), 56.1 ($NCH_2CH_2CH_2N$), 60.3 ($ArCH_2N$), 120.6 (Ar–C), 124.7 (Ar–C), 128.4 (Ar–CH), 129.6 (Ar–C), 131.3 (Ar–CH), 158.6 (Ar–CO); $^{119}Sn\{^1H\}$ NMR (186 MHz, CD_2Cl_2, 298 K) δ_{Sn}: −475; elemental analysis calculated for $C_{23}H_{30}N_2O_2Sn$: C, 56.93; H, 6.23; N, 5.77; Found C, 56.23; H, 6.23; N, 5.22.

Synthesis of [{L^6}Sn$_2$]·Py$_2$ (5). H_4L^4 (0.597 g, 1 mmol) was added to $Sn(HMDS)_2$ (0.88 g, 2 mmol) in pyridine, at 0 °C. The reaction mixture was left stirring for one hour. It was concentrated *in vacuo*, and the product was recrystallised from pyridine. Yield = 82%. ^1H NMR (500 MHz, Pyr-d^5, 298 K) δ_H: 2.12 (s, 12H, Ar4CH_3), 2.22 (s, 12H, Ar–CH_3), 3.50 (s, 4H, NCH_2CH_2N), 3.79 (d w/shouldering, 4H, Ar–CH_2N), 3.97 (m, 4H, Ar–CH_2N), 6.79 (d, J = Hz, 4H, Ar–H), 6.99 (d, J = Hz, 4H, Ar–H), 7.19 (m 8H, *m*-C_5H_5N), 7.55 (m 4H, *p*-C_5H_5N), 8.70 (m 8H, *o*-C_5H_5N); $^{13}C\{^1H\}$ NMR (126 MHz, 25 °C); δ_{ppm} 18.2 (Ar–Me), 20.0 (Ar–Me), 48.7 (NCH_2CH_2N), 55.9 (Ar–CH_2N), 124.1 (*m*-C_5H_5N), 124.5 (Ar–C) 125.9, (Ar–CH), 129.2 (Ar–C), 130.1 (Ar–C), 132.6 (Ar–CH), 136.2 (Ar–C), 136.1 (*p*-C_5H_5N), 150.4 (*o*-C_5H_5N), 150.0, 158.7 (Ar–CO); ^{119}Sn NMR (186 MHz, 25 °C); δ_{ppm} −532; ^{119}Sn NMR (125 MHz, C_6D_6, 25 °C); δ_{ppm} −477; elemental analysis for $C_{48}H_{54}N_4O_4Sn_2$: calc. C, 58.33; H, 5.51; N, 5.67; Found C, 58.31; H, 5.18; N, 5.61.

Synthesis of [{L^1}$_2$Sn] (6). Complex **1** (1 mmol, 0.4321 g) was dissolved in toluene (20 mL) and cooled to 0 °C before a stream of oxygen was bubbled through the solution. The solution was stirred for 30 minutes. The solvent was removed *in vacuo*, and 10 ml of fresh toluene was used to extract the residue. The reaction mixture was filtered through Celite and concentrated *in vacuo* (5 ml). The product was recrystallised from toluene at −5 °C. Yield, 0.32 g (44%). Elemental analysis calculated for $C_{40}H_{50}N_2O_4Sn$: C, 64.78; H, 6.80; N, 3.78; Found C, 60.26; H, 5.91; N, 3.29.0. ^1H NMR (500 MHz, CD_2Cl_2, 298 K) δH 1.03 (m, 6H, NCH_2CH_3), 1.46 (s, 6H, Ar–Me), 2.18 (s, 6H, Ar–Me), 2.20 (s, 6H, Ar–Me), 2.22 (s, 6H, Ar–Me), 2.98 (m, 2H, NCH_2CH_3), 3.16 (m, 2H, NCH_2CH_3), 3.63 (m, 4H, $ArCH_2N$), 5.10 (q, J = 13.0 Hz, 2H, $ArCH_2N$), 5.33 (q, J = 13.0 Hz, 2H, $ArCH_2N$), 6.70 (s, 2H, ArH), 6.77 (s, 2H, ArH), 6.83 (s, 2H, ArH), 6.90 (s, 2H, ArH); $^{13}C\{^1H\}$ NMR (125 MHz, CD_2Cl_2, 298 K) δC: 4.70 (NCH_2CH_3), 16.4 (Ar–Me), 17.4 (Ar–Me), 20.4 (Ar–Me), 20.5 (Ar–Me), 44.2 (NCH_2CH_3), 56.4 ($ArCH_2N$), 57.2 ($ArCH_2N$), 119.1 (Ar–C), 120.6 (Ar–C), 126.3 (Ar–C), 126.9 (Ar–C), 127.7 (Ar–C), 128.4 (Ar–CH), 128.5 (Ar–CH), 129.0 (Ar–C), 131.9 (Ar–CH), 132.2 (Ar–CH), 157.6 (Ar–CO), 157.6 (Ar–CO); ^{119}Sn NMR (186 MHz, CD_2Cl_2, 298 K) δSn: −670.

Crystallographic details

Single crystal X-ray diffraction data were collected on a SuperNova, EosS2 diffractometer using CuKα (λ = 1.54184 Å) radiation, except for **1** which was collected using MoKα (λ = 0.71073 Å) radiation. In each case, the crystals were maintained at 150 K during data collection. Using Olex2, the structures were solved with the olex2. solve structure solution program or ShelXT and refine with the ShelXL refinement package using least–squares minimisation.

Table 1 contains crystal and structural refinement data for **1**, **2**, **3**, **5** and **6**. The SI contains data for the {^{t}Bu} analogue of **3** (^{t}Bu$_4$Sn).

Conclusions

A series of Sn(II) complexes (**1–5**) bearing amine bis(phenolate) were obtained cleanly in quantitative yields, having different steric crowding around the metal, and their structures were confirmed by X-ray crystallography. The [O^N^O]-type ligands {**L^1**} and {**L^6**} bind to the metal in a tridentate fashion. In the case of **1**, the {**L^1**} bridges to Sn(II) centres. On the other hand, in the [O^N^O–N]-ligands, {**L^2**}, and [O^N^N^O]-ligands, {**L^3**}–{**L^4**} bind to the metal centres in a tetradentate fashion. In the case of the pre-ligand L^5H_2, reaction with $Sn(HMDS)_2$ did not yield tractable products.

Single crystal X-ray diffraction studies of the direct reaction of **1** with O_2 reveal the formation of a Sn(IV) complex, presumably by a ligand exchange process, with concomitant formation of SnO_2.

Taken together, these efforts demonstrate the complex coordination behaviour and utility of the ligands in terms of producing controlled structured $M(OR)_2$ systems. Further development of these types of ligands will facilitate controlled construction of even more complex $M(OR)_x$ systems for materials applications.

Author contributions

Conceptualization, A. L. J.; methodology, A. R. and H. dL.; crystallography, A. L. J. and G. K. K.; writing—draft preparation, A. L. J.; writing—review/editing, A. L. J.; supervision, A. L. J.; project administration, A. L. J.; and funding acquisition, A. L. J. All authors have read and agreed to the published version of the manuscript.

Conflicts of interest

There are no conflicts to declare.

Data availability

The data that support the findings of this study are available in the SI of this article. General experimental details, the synthesis of [^{t}Bu$_4$Sn] and crystallographic data for [^{t}Bu$_4$Sn]; experimental details of the data collection/X-ray crystallographic studies of **1–6** and [**^{t}Bu$_4$Sn**]; and characterisation data for the {^{t}Bu} analogue of **3**, **^{t}Bu$_4$Sn**. See DOI: **https://doi.org/10.1039/d5dt01442e**.

CCDC 2465589–2465595 contain the supplementary crystallographic data for this paper.[66a–g]

Where possible, additional data that support the findings of this study are available from the corresponding authors upon reasonable request.

References

1 P. J. Davidson and M. F. Lappert, *J. Chem. Soc., Chem. Commun.*, 1973, 317–317.
2 Y. Mizuhata, T. Sasamori and N. Tokitoh, *Chem. Rev.*, 2009, **109**, 3479–3511.
3 M. Asay, C. Jones and M. Driess, *Chem. Rev.*, 2010, **111**, 354–396.
4 L. Álvarez-Rodríguez, J. A. Cabeza, P. García-Álvarez and D. Polo, *Coord. Chem. Rev.*, 2015, **300**, 1–28.
5 N. Tokitoh and R. Okazaki, *Coord. Chem. Rev.*, 2000, **210**, 251–277.
6 J. Baumgartner and C. Marschner, *Rev. Inorg. Chem.*, 2014, **34**, 119–152.
7 A. V. Zabula and F. E. Hahn, *Eur. J. Inorg. Chem.*, 2008, **2008**, 5165–5179.
8 T. Chu and G. I. Nikonov, *Chem. Rev.*, 2018, **118**, 3608–3680.
9 S. Yadav, S. Saha and S. S. Sen, *ChemCatChem*, 2016, **8**, 486–501.
10 D. Sarkar, C. Weetman, D. Munz and S. Inoue, *Angew. Chem., Int. Ed.*, 2020, **60**, 3519–3523.
11 Y. Peng, B. D. Ellis, X. Wang and P. P. Power, *J. Am. Chem. Soc.*, 2008, **130**, 12268–12269.
12 D. M. Barnhart, D. L. Clark and J. G. Watkin, *Acta Crystallogr., Sect. C:Cryst. Struct. Commun.*, 1994, **50**, 702–704.
13 B. Cetinkaya, I. Gumrukcu, M. F. Lappert, J. L. Atwood, R. D. Rogers and M. J. Zaworotko, *J. Am. Chem. Soc.*, 2002, **102**, 2088–2089.
14 C. Stanciu, A. F. Richards, M. Stender, M. M. Olmstead and P. P. Power, *Polyhedron*, 2006, **25**, 477–483.
15 D. A. Dickie, I. S. MacIntosh, D. D. Ino, Q. He, O. A. Labeodan, M. C. Jennings, G. Schatte, C. J. Walsby and J. A. C. Clyburne, *Can. J. Chem.*, 2008, **86**, 20–31.
16 T. J. Boyle, T. Q. Doan, L. A. M. Steele, C. Apblett, S. M. Hoppe, K. Hawthorne, R. M. Kalinich and W. M. Sigmund, *Dalton Trans.*, 2012, 41.
17 M. G. Davidson, C. L. Doherty, A. L. Johnson and M. F. Mahon, *Chem. Commun.*, 2003, 1832–1833.
18 T. J. Boyle, H. D. Pratt, L. A. M. Ottley, T. M. Alam, S. K. McIntyre, M. A. Rodriguez, J. Farrell and C. F. Campana, *Inorg. Chem.*, 2009, **48**, 9191–9204.
19 K. V. Zaitsev, E. A. Kuchuk, A. V. Churakov, M. A. Navasardyan, M. P. Egorov, G. S. Zaitseva and S. S. Karlov, *Inorg. Chim. Acta*, 2017, **461**, 213–220.
20 K. V. Zaitsev, E. A. Kuchuk, A. V. Churakov, G. S. Zaitseva, M. P. Egorov and S. S. Karlov, *Russ. Chem. Bull.*, 2017, **66**, 622–627.
21 S. Praban, S. Yimthachote, J. Kiriratnikom, S. Chotchatchawankul, J. Tantirungrotechai and K. Phomphrai, *J. Polym. Sci., Part A: Polym. Chem.*, 2019, **57**, 2104–2112.
22 B. N. Mankaev, V. A. Serova, M. A. Syroeshkin, A. Y. Akyeva, A. V. Sobolev, A. V. Churakov, E. K. Lermontova, M. E. Minyaev, Y. F. Oprunenko, M. V. Zabalov, K. V. Zaitsev, G. S. Zaitseva and S. S. Karlov, *Eur. J. Inorg. Chem.*, 2023, **26**, e202200690.
23 P. Piromjitpong, P. Ratanapanee, W. Thumrongpatanaraks, P. Kongsaeree and K. Phomphrai, *Dalton Trans.*, 2012, **41**, 12704–12710.
24 S. V. Baryshnikova, E. V. Bellan, A. I. Poddel'sky, G. K. Fukin and G. A. Abakumov, *Inorg. Chem. Commun.*, 2016, **69**, 94–97.
25 S. Yimthachote, P. Chumsaeng and K. Phomphrai, *Dalton Trans.*, 2022, **51**, 509–517.
26 D. A. Atwood, J. A. Jegier, K. J. Martin and D. Rutherford, *J. Organomet. Chem.*, 1995, **503**, C4–C7.
27 N. N. Zemlyansky, I. V. Borisova, M. G. Kuznetsova, V. N. Khrustalev, Y. A. Ustynyuk, M. S. Nechaev, V. V. Lunin, J. Barrau and G. Rima, *Organometallics*, 2003, **22**, 1675–1681.
28 M. C. Kuchta, J. M. Hahn and G. Parkin, *J. Chem. Soc., Dalton Trans.*, 1999, 3559–3563, DOI: **10.1039/a905490a**.
29 M. Westerhausen, S. Schneiderbauer, A. N. Kneifel, Y. Söltl, P. Mayer, H. Nöth, Z. Zhong, P. J. Dijkstra and J. Feijen, *Eur. J. Inorg. Chem.*, 2003, **2003**, 3432–3439.
30 H. Jing, S. K. Edulji, J. M. Gibbs, C. L. Stern, H. Zhou and S. T. Nguyen, *Inorg. Chem.*, 2004, **43**, 4315–4327.
31 R. Gericke and J. Wagler, *Main Group Met. Chem.*, 2014, **37**, 1–9.
32 B. M. Barry, B. W. Stein, C. A. Larsen, M. N. Wirtz, W. E. Geiger, R. Waterman and R. A. Kemp, *Inorg. Chem.*, 2013, **52**, 9875–9884.
33 J. C. Machell, D. M. P. Mingos and T. L. Stolberg, *Polyhedron*, 1989, **8**, 2933–2935.
34 A. V. Piskunov, A. V. Lado, G. K. Fukin, E. V. Baranov, L. G. Abakumova, V. K. Cherkasov and G. A. Abakumov, *Heteroat. Chem.*, 2006, **17**, 481–490.
35 H. S. I. Sullivan, A. J. Straiton, G. Kociok-Köhn and A. L. Johnson, *Inorganics*, 2022, **10**(9), 129.
36 R. Kuriki, T. Kuwabara and Y. Ishii, *Dalton Trans.*, 2020, **49**, 12234–12241.
37 T. Hascall, G. Parkin, T. Hascall, A. L. Rheingold and I. Guzei, *Chem. Commun.*, 1998, 101–102, DOI: **10.1039/a705937j**.
38 T. Hascall, K. Pang and G. Parkin, *Tetrahedron*, 2007, **63**, 10826–10833.
39 B. G. McBurnett and A. H. Cowley, *Chem. Commun.*, 1999, 17–18, DOI: **10.1039/a807167e**.
40 O. Wichmann, R. Sillanpää and A. Lehtonen, *Coord. Chem. Rev.*, 2012, **256**, 371–392.
41 A. J. Straiton, C. L. McMullin, G. Kociok- Köhn, C. L. Lyall, J. D. Parish and A. L. Johnson, *Inorg. Chem.*, 2023, **62**, 2576–2591.
42 D. Mondal, S. Kundu, M. C. Majee, A. Rana, A. Endo and M. Chaudhury, *Inorg. Chem.*, 2017, **56**, 9448–9460.
43 W. Clegg, M. G. Davidson, D. V. Graham, G. Griffen, M. D. Jones, A. R. Kennedy, C. T. O'Hara, L. Russo and C. M. Thomson, *Dalton Trans.*, 2008, 1295–1301.
44 A. L. Johnson, M. G. Davidson, Y. Pérez, M. D. Jones, N. Merle, P. R. Raithby and S. P. Richards, *Dalton Trans.*, 2009, DOI: **10.1039/b904534a**.
45 S. L. Hancock, M. F. Mahon, G. Kociok–Kőhn and M. D. Jones, *Eur. J. Inorg. Chem.*, 2011, **2011**, 4596–4602.

46 S. L. Hancock, M. F. Mahon and M. D. Jones, *Dalton Trans.*, 2011, **40**, 2033–2037.
47 E. Y. Tshuva, I. Goldberg, M. Kol and Z. Goldschmidt, *Inorg. Chem.*, 2001, **40**, 4263–4270.
48 S. M. Malathy Sony, M. Kuppayee, M. N. Ponnuswamy, J. Manonmani, M. Kandasamy and H.-K. Fun, *Cryst. Res. Technol.*, 2002, **37**, 1360–1367.
49 T. Berends, L. Iovkova, G. Bradtmöller, I. Oppel, M. Schürmann and K. Jurkschat, *Z. Anorg. Allg. Chem.*, 2009, **635**, 369–374.
50 L. Iovkova–Berends, T. Berends, T. Zöller, G. Bradtmöller, S. Herres–Pawlis and K. Jurkschat, *Eur. J. Inorg. Chem.*, 2012, **2012**, 3191–3199.
51 L. Iovkova–Berends, T. Berends, T. Zöller, D. Schollmeyer, G. Bradtmöller and K. Jurkschat, *Eur. J. Inorg. Chem.*, 2012, **2012**, 3463–3473.
52 F. Wolff, C. Lorber, R. Choukroun and B. Donnadieu, *Eur. J. Inorg. Chem.*, 2004, **2004**, 2861–2867.
53 D. L. Coward, B. R. M. Lake, R. Poli and M. P. Shaver, *Macromolecules*, 2019, **52**, 3252–3256.
54 H. C. Quilter, R. H. Drewitt, M. F. Mahon, G. Kociok-Köhn and M. D. Jones, *J. Organomet. Chem.*, 2017, **848**, 325–331.
55 M. Mijanuddin, A. D. Jana, M. G. B. Drew, C. S. Hong, B. Chattopadhyay, M. Mukherjee, M. Nandi, A. Bhaumik, M. Helliwell, G. Mostafa and M. Ali, *Polyhedron*, 2009, **28**, 665–672.
56 A. W. Addison, T. N. Rao, J. Reedijk, J. van Rijn and G. C. Verschoor, *J. Chem. Soc., Dalton Trans.*, 1984, 1349–1356, DOI: **10.1039/dt9840001349**.
57 K. Ambrose, J. N. Murphy and C. M. Kozak, *Inorg. Chem.*, 2020, **59**, 15375–15383.
58 L. E. H. Paul, I. C. Foehn, A. Schwarzer, E. Brendler and U. Böhme, *Inorg. Chim. Acta*, 2014, **423**, 268–280.
59 N. Srivastav, R. Singh, V. Kaur, J. Wagler and E. Kroke, *Inorg. Chim. Acta*, 2017, **463**, 54–60.
60 K. Jurkschat, N. Pieper, S. Seemeyer, M. Schürmann, M. Biesemans, I. Verbruggen and R. Willem, *Organometallics*, 2001, **20**, 868–880.
61 Q. Sun, Y. Wang, D. Yuan, Y. Yao and Q. Shen, *Dalton Trans.*, 2015, **44**, 20352–20360.
62 M. Abid, R. Nouch, T. D. Bradshaw, W. Lewis and S. Woodward, *Eur. J. Inorg. Chem.*, 2019, **2019**, 2774–2780.
63 L.-C. Liang, C.-C. Chien, M.-T. Chen and S.-T. Lin, *Inorg. Chem.*, 2013, **52**, 7709–7716.
64 A. J. Chmura, M. G. Davidson, M. D. Jones, M. D. Lunn and M. F. Mahon, *Dalton Trans.*, 2006, 887–889, DOI: **10.1039/b513345a**.
65 T. Fjeldberg, H. k. Hope, M. F. Lappert, P. P. Power and A. J. Thorne, *J. Chem. Soc., Chem. Commun.*, 1983, 639–641.
66 (*a*) A. L. Johnson and A. Ryan, CCDC 2465589: Experimental Crystal Structure Determination, 2024, DOI: **10.5517/ccdc.csd.cc2nrn47**; (*b*) A. L. Johnson and A. Ryan, CCDC 2465590: Experimental Crystal Structure Determination, 2024, DOI: **10.5517/ccdc.csd.cc2nrn58**; (*c*) A. L. Johnson and A. Ryan, CCDC 2465591: Experimental Crystal Structure Determination, 2024, DOI: **10.5517/ccdc.csd.cc2nrn69**; (*d*) A. L. Johnson and A. Ryan, CCDC 2465592: Experimental Crystal Structure Determination, 2024, DOI: **10.5517/ccdc.csd.cc2nrn7b**; (*e*) A. L. Johnson and A. Ryan, CCDC 2465593: Experimental Crystal Structure Determination, 2024, DOI: **10.5517/ccdc.csd.cc2nrn8c**; (*f*) A. L. Johnson and A. Ryan, CCDC 2465594: Experimental Crystal Structure Determination, 2024, DOI: **10.5517/ccdc.csd.cc2nrn9d**; (*g*) A. L. Johnson and A. Ryan, CCDC 2465595: Experimental Crystal Structure Determination, 2024, DOI: **10.5517/ccdc.csd.cc2nrnbf**.